

Characterization of Chaos in a Hybrid Optically Bistable Device

F. A. Hopf, D. L. Kaplan, M. H. Rose, and L. D. Sanders

Optical Sciences Center, Tucson, Arizona 85721

and

M. W. Derstine

Honeywell, Inc., Bloomington, Minnesota 55420

(Received 16 June 1986)

Dimension and correlation entropy are measured for various settings of our hybrid optically bistable device. Measured dimension is found to be significantly less than dimensions consistent with the Kaplan-Yorke conjecture. The standard method of determining correlation entropy is shown to yield more than one value.

PACS numbers: 05.45.+b, 42.65.Pc

Recently, a repertoire of tools for the recognition and analysis of chaos has included various empirical techniques for the estimation of dimension¹ of an attractor and various entropies from a time series. Current techniques involve (1) estimation of a dimension from the Kaplan-Yorke (KY) conjecture (limited to theory²), (2) estimation of the dimension from an embedding procedure (experiment³ and theory⁴), (3) estimation of a correlation entropy from the embedding (mostly experimental⁵), and (4) estimation of the trajectory divergence directly (experiment⁶ and theory⁴). The techniques involving embeddings have met with success in several cases of low dimensionality.⁷

In this paper we experimentally verify the existence of few-dimensional chaos in our device by using embedding techniques and by directly measuring trajectory divergences. We find that methods (1) and (2) are inconsistent in this case, and method (3) gives multivalued results whose meaning must be sorted out through use of a modified version of (4). The KY conjecture requires a dimensionality greater than two, where two is the minimum number of nonnegative Lyapunov exponents needed to describe chaos. We find $\nu < 2$ over broad parameter ranges (ν denotes our measured dimensionality).

Our device is illustrated in Fig. 1. The beam from a helium-neon laser passes through a modulator [polarizer and potassium dihydrogen phosphate (KDP) crystal] and is coupled into an optical fiber. The light emerging from the fiber is detected with a photomultiplier, and an amplified electrical signal is applied to the KDP crystal, thereby achieving delayed feedback. The system is modeled by the differential delay equation⁸

$$\tau dX(t)/dt + X(t) = \mu \pi \{ 1 - \xi \cos[X(t - t_R) + X_B] \}. \quad (1)$$

Here $X = -\pi V/V_h$, V is the voltage applied to the modulator, V_h is the half-wave voltage of the modulator, and $X_b = \pi V_b/V_h$ is a variable bias which is set equal to $-\pi/2$. The quantity μ is proportional to the product of the input laser intensity and the total amplifier gain; μ serves as the bifurcation parameter in our experiment. The ability of the system to achieve extinction is measured by $\xi = 0.96 \pm 0.01$. We use two values of t_R/τ : "fast" ($t_R/\tau = 6 \pm 1$) and "slow" ($t_R/\tau = 3 \pm 0.5$), where the relative terms "fast" and "slow" pertain to this experiment. The fiber delay $t_R = 6 \mu s$ sets the fundamental period (or periodic component) equal to $2(t_R + \delta)$ where $0 < \delta \leq \tau$ and δ depends on μ . The device bifurcates to chaos through a Feigenbaum period-doubling sequence that is truncated by noise.⁹ The period-two, -four, and -eight wave forms are denoted P_2 , P_4 , and P_8 . In the chaotic regime the periodic structure is lost in inverse order with wave forms denoted N_8 , N_4 , and N_2 . We study only the inverse sequence since in this domain the chaos is unique and well characterized.^{9,10} Wave

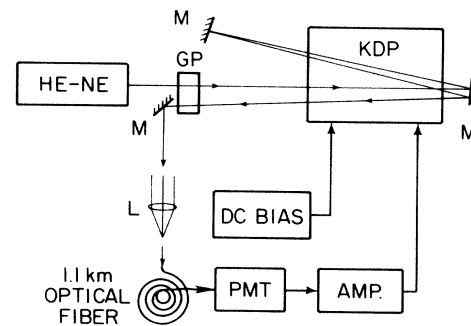


FIG. 1. Experimental layout: He-Ne laser; GP, Glan prism, KDP, crystal; M, mirrors; PMT, photomultiplier; L, lens.

forms whose data appear here were chosen by operation at the low μ end of the N_n domain. This locates the operating point more accurately than specification of μ , whose error is of the order of the N_4 domain.

A transient digitizer measures the voltage V at the amplification stage in intervals t_s , and stores it in the form $V_i = V(t_i)$, $t_i = it_s$, $i = 1-26\,000$. We construct vectors $V_{d,i} = (V(t_i), V(t_i + mt_s), V(t_i + 2mt_s), \dots, V(t_i + mdt_s))$, where d is the embedding dimension and m is some integer. We show results for $m = 1$ but have obtained the same results for larger m . We calculate correlation¹¹ integrals $C_d(\epsilon)$, i.e., the number of pairs of vectors whose Euclidean separation $|V_{d,i} - V_{d,j}|$ is less than the distance ϵ . For a chaotic signal⁵

$$\ln[C_d(\epsilon)] \propto \nu \ln[\epsilon] + K_c dt_s. \quad (2)$$

We use the terms dimension (ν) and correlation entropy (K_c) to describe our results whenever their use is consistent with the data.

The embedding compares a set of M vectors against a set of N , where we typically choose $M = N = 1200$. When we test M or N beyond this value (up to 3500) we see little improvement in the results because the "signal to noise" properties of the embedding increase logarithmically with M or N . Figure 2 (top) shows embeddings of a "slow" N_4 (left) and a "fast" N_2 (right) wave form. $\log_2 C_d(\epsilon)$ is plotted versus $\log_2 \epsilon$ for $d = 1-6, 9, 12, 15, 18$. In the middle row of Fig. 2 we show the slopes ν_d of $C_d(\epsilon)$ computed between values of $C_d(\epsilon)$ indicated by the heavy arrows on the right-hand borders of the top figures. The slopes are computed by a regression analysis. The estimates of the 2σ points, shown as dots, suggest the linearity of the correlation curves, but are unclear error estimates because the points in the embedding are not statistically independent. We estimate our random error by twenty independent embeddings, which yields less than 5% variation in ν (we do not know of definitive work on systematic errors¹²). Note that for $d > 7$ the slopes ν_d converge to a value ν , our estimate of the dimension, which supports the suggested rule¹² that dimension should be determined at a minimum $d \approx 2\nu + 1$. Observe that $\nu = 1.6$ in the left column, and $\nu = 2.8$ on the right. The "slow" N_2 has $\nu = 1.9$; the "fast" N_4 has $\nu = 1.8$.

Vallée and Delisle¹³ have visualized this change in dimensionality (from $\nu < 2$ to $\nu > 2$) in a device similar to ours using the Poincaré section¹⁴ which we obtain by synchronizing t_s with t_R by means of a phase-locking device. The Poincaré sections of the wave forms are shown at the bottom of Fig. 2. The one to the left is linelike, while the one to the right is considerably broader, suggesting a filling out of the phase space. The finite width of our section (left) is the same as the scatter obtained from the section of a

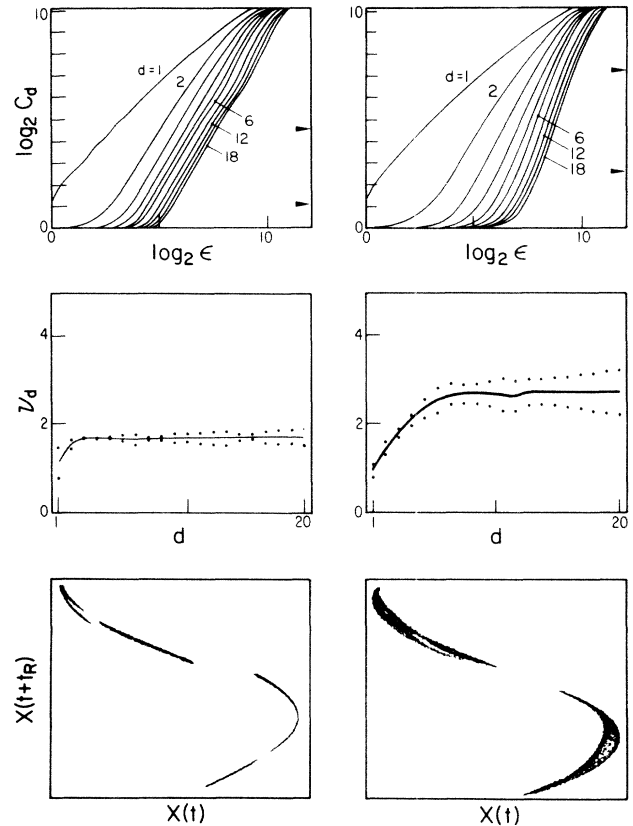


FIG. 2. Top: Correlation integrals, $\log_2 C_d$ vs $\log_2 \epsilon$, for "slow" N_4 (left) and "fast" N_2 (right). Plots for $d = 1-6, 9, 12, 15, 18$ are shown. Slopes computed between heavy arrows on right borders of the top figures. Center: Slope ν , obtained by a line fit of each curve above. Dots indicate uncertainty in line fit. N_4 has $\nu < 2$. Bottom: Poincaré sections of N_4 and N_2 . Linelike (suggesting $\nu \leq 1$) N_4 section on left; filled out ($\nu > 1$) section on right. For simplicity, period is denoted by $2t_R$ (see text).

periodic signal, indicating that the spread is due to synchronization noise. This noise prevents us from obtaining good straight lines when we embed⁵ the Poincaré section. The common noise factor indicates that we can embed a section of a periodic signal to test for the minimum ϵ for which a dimension¹⁵ of zero can be observed. Within the specified range of ϵ , we obtain a dimension that is approximately $\nu - 1$ from the chaotic traces. The values $\nu - 1 < 1$ are close to the values obtained when Eq. (1) is reduced to a one-dimensional map whose iterates are tested by the embedding.

Figure 3 is a plot of the family of curves $[\log_2 C_d(\epsilon) - \log_2 C_{d+1}(\epsilon)]/mt_s$ vs d for all ϵ over the same portion of the embedding shown in Fig. 1 that is used to compute the dimension ($t_s = 1 \mu s$, $m = 1$, $d < 20$). A correlation entropy⁵ exists if for some range of d and independent of ϵ these curves converge on a constant K_c . To verify that we can resolve such a

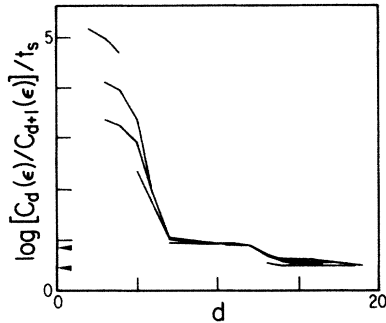


FIG. 3. Plot of family of curves $[\log_2 C_d(\epsilon) - \log_2 C_{d+1}(\epsilon)]/t_s$ vs d for all ϵ over same portion of embedding shown in Fig. 1 ($t_s = 1 \mu\text{s}$, $d < 20$).

constant, we test periodic and noisy signals and observe no convergence. As Fig. 3 shows, we find that two convergences occur, one for $8 < d < 12$ and another for $14 < d < 20$. We have observed (by varying m) the empirical relationship $mt_s K d_{\max} = c$. Here K is some plateau, d_{\max} is the maximum d for which it may be observed, and c is a constant for any one wave form (varies between wave forms over a range $1 < c < 2$). Both plateaus in Fig. 3 vanish at their appropriate d_{\max} . Neither convergence can be taken to be more fundamental than the other.

To understand the origin of these plateaus, we estimate trajectory divergences.⁶ We search the data set for points near V_i which generate a subset $\{V_j\}$ such that for all j and for $n=0, \dots, n_{\max}$, $|V(it_s + nt_s) - V(jt_s + nt_s)| < V_0$. Here V_0 is 0.4% of the maximum voltage variation. As prohibitively few such subsets occur in the asynchronous data, we use the synchronous data which typically yields 100 such subsets for $n_{\max}=1$. We then compute the standard deviations $\sigma_i(ut_s)$, $u = n - n_{\max} = 0, 1, \dots$, of the set of voltages. If it exists, we estimate the "local trajectory divergence" rate γ_i^+ at $t = it_s$ as the exponential rate of increase of $\sigma_i(ut_s)$ with $t = ut_s$. We estimate the trajectory divergence rate γ^+ using the exponential rate of increase of $\langle \sigma_i(ut_s) \rangle_i$ with $t = ut_s$ ($\langle \rangle_i$ signifies average over i). For the data in Fig. 3, $\gamma^+ = 0.4$, which agrees with the lower plateau ($14 < d < 20$) in Fig. 3 and with the local divergence rates measured here and earlier.¹⁶

Because $C_d(\epsilon)$ is unchanged if $t_s \rightarrow -t_s$, we are motivated to subject the data to time reversal and repeat the analysis described above, now looking for an "effective average convergence." As above, we examine the way in which nearby trajectories (now time reversed) depart from each other. Results from the N_2 data are similar to results obtained when a map¹⁷ derived from Eq. (1) (in the domain of N_2 ; the logistics map is similarly tested) is iterated to form a se-

quence and then time reversed. The plot of $\log \langle \sigma_i \rangle_i$ vs t is linear for both cases, yielding an effective average trajectory convergence rate denoted γ^- . Both γ^- 's are about twice their respective γ^+ 's. We fail to obtain in either case a local convergence rate γ_i^- for all but a negligible subset of i 's. Instead we typically observe that $\sigma_i(ut_s)$ is a step function. For the data in Fig. 3, $\gamma^- = 0.8$, which agrees with the upper plateau ($8 < d < 12$). The rates γ^+ and γ^- are indicated on the ordinate of Fig. 3.

Since the map is chaotic and has one degree of freedom, we can be sure that its γ^- is not associated with a Lyapunov exponent. Our device is no different from the map in its local convergence properties, and so we suspect that γ^- in our system is also not associated with an exponent. Furthermore, the agreement between γ^+ and our lower plateau suggests that we have only one positive Lyapunov exponent.¹⁸ The pointwise analysis thus allows us uniquely to associate a Lyapunov exponent with the average divergence rate and its corresponding value of the correlation entropy. If chaos is a stationary process then the rate at which trajectories leave a volume of phase space must be balanced by a rate at which they are brought into the volume. If the rate at which trajectories leave the volume is determined by the Lyapunov exponents, then the rate implied by γ^- , an object that is fabricated by the averaging, implies, in our system, an imbalance of the rates of convergence and divergence. It follows that the effective average convergence is not, even on the average, the same kind of process as the divergence.

In summary, we have explored various methods for recognition and characterization of chaos. We have found the embedding to be a powerful tool for establishing the qualitative claim that erraticism in our system is due to deterministic rather than stochastic processes.¹⁹ We are unable to offer unqualified support for quantitative applications. We observe a dimension qualitatively less than that of KY. Figure 4 of Ref. 1 indicates that such discrepancies are possible mathematically. We believe that we are observing a similar discrepancy in a real system. We see substantial changes in measured dimension in the N_n domains without correlated changes in other properties of the system. Other experimental^{14,20} and theoretical²¹ groups have extensively studied the same (chaotic) domains and fail to report any abrupt physical changes associated with the transition in dimension from less than two to greater than two. Especially in our slower system, all the spectral properties and all of the rates vary smoothly through this transition, offering indirect support for the notion of an underlying dimensionality that has physical significance but which might resist measurement. We feel that it is premature to claim that our value $\nu > 2$ measures this dimensionality. We

obtain at least two values of the correlation entropy, neither of which can be taken as correct on the basis of inspection of the embedding alone. We have determined from trajectory divergence analyses that one represents an average divergence rate and another an effective average convergence rate. We have found similar rates in mappings, verifying that there can be more rates than Lyapunov exponents. The Lyapunov exponents require averaging over the attractor in order for them to be well-defined constants. When chaos is investigated by examination of average properties of the attractor, excess rates are fabricated by the averaging. By investigating pointwise properties of the system we can objectively identify which rates are Lyapunov exponents and which are fabrications.

The authors acknowledge private communications with J. D. Farmer and I. Procaccia, and the support of the National Science Foundation (Grant No. PHY-8408259).

¹J. D. Farmer, in *Evolution of Order and Chaos*, edited by H. Haken (Springer-Verlag, New York, 1982), p. 228, notes that there is a potentially confusing nomenclature in the literature associated with dimensions. There are multiplicities of definitions and interrelationships are conjectured. Similar problems exist with entropies. We therefore adopt a neutral approach to terminology in this paper. Farmer (private communication) states that our ν (called correlation exponent) estimates the information dimension.

²J. Kaplan and J. Yorke, *Functional Differential Equations and Approximation of Fixed Points* (Springer-Verlag, New York, 1979), p. 204.

³A. Brandstätter, J. Swift, H. L. Swinney, A. Wolf, J. D. Farmer, E. Jen, and P. J. Crutchfield, *Phys. Rev. Lett.* **51**, 1442 (1983); M. Giglio, S. Musazzi, and U. Perini, *Phys. Rev. Lett.* **53**, 2402 (1984).

⁴N. H. Packard, J. P. Crutchfield, J. D. Farmer, and R. S. Shaw, *Phys. Rev. Lett.* **45**, 712 (1980).

⁵G. P. Puccioni, A. Poggi, W. Gadomski, J. R. Tredicce, and F. T. Arecchi, *Phys. Rev. Lett.* **55**, 339 (1985); A. M. Albano, J. Abounadi, T. H. Chyba, C. E. Searle, S. Young, R. S. Gioggia, and N. B. Abraham, *J. Opt. Soc. Am. B* **2**, 47 (1985); for tests see P. Grassberger and I. Procaccia, *Phys. Rev. A* **28**, 2591 (1983).

⁶J. P. Gollub, E. J. Romer, and J. E. Socolar, *J. Stat. Phys.* **23**, 321 (1980).

⁷J. D. Farmer, *Physica (Amsterdam)* **4D**, 366 (1982).

⁸K. Ikeda, *Opt. Commun.* **30**, 257 (1979); K. Ikeda, H. Daido, and O. Akimoto, *Phys. Rev. Lett.* **45**, 709 (1980).

⁹M. W. Derstine, H. M. Gibbs, F. A. Hopf, and D. L. Kaplan, *Phys. Rev. A* **26**, 3720 (1982).

¹⁰M. W. Derstine, H. M. Gibbs, F. A. Hopf, and D. L. Kaplan, *Phys. Rev. A* **25**, 3200 (1983).

¹¹P. Grassberger and I. Procaccia, *Phys. Rev. Lett.* **50**, 346 (1983).

¹²J. Holzfuss and G. Mayer-Kress, to be published.

¹³R. Vallée and C. Delisle, poster session at *Optical Bistability III*, edited by H. M. Gibbs *et al.* (Springer-Verlag, New York, 1986).

¹⁴H. L. Swinney, *Physica (Amsterdam)* **7D**, 3 (1983).

¹⁵J.-C. Roux, R. H. Simoyi, and H. L. Swinney, *Physica (Amsterdam)* **8D**, 257 (1983), note that the dimension of the Poincaré section is slightly greater than $\nu - 1$.

¹⁶M. W. Derstine, H. M. Gibbs, F. A. Hopf, and L. D. Sanders, *IEEE J. Quantum Electron.* **21**, 1419 (1985).

¹⁷J. Carr and J. C. Eilbeck, *Phys. Lett.* **104A**, 59 (1984).

¹⁸J. B. Pesin, *Russian Math. Surveys* **32**, 455 (1977); J.-P. Eckmann and D. Ruelle, *Rev. Mod. Phys.* **57**, 617 (1985).

¹⁹F. A. Hopf, *Phys. Rev. Lett.* **56**, 2800 (1986).

²⁰M. Okada and K. Takizawa, *IEEE J. Quantum Electron.* **17**, 2135 (1981); Li-xue Chen, Chun-fei Li, and Jing Hong, in Ref. 13, p. 323.

²¹K. Ikeda, *J. Phys. (Paris)*, *Colloq.* **44**, C2-183 (1983); J. Y. Gao, L. M. Narducci, H. Sadiky, M. Squicciarini, and J. M. Yuan, *Phys. Rev. A* **30**, 901 (1984).